Isomorphous Substitution of Transition-Metal Ions in the Nanoporous Nickel Phosphate VSB-5

Sung Hwa Jhung,[†] Jong-San Chang,*[,†] Young Kyu Hwang,[†] Jean-Marc Grenèche,[‡] Gérard Férey,[§] and Anthony K. Cheetham*[,||]

Research Center for Nanocatalysts, Korea Research Institute of Chemical Technology, P.O. Box 107, Yusung, Daejeon 305-600, Korea, Laboratoire de Physique de l'Etat Condensé, Université du Maine, 72000 Le Mans, France, Institut Lavoisier, UMR CNRS 173, Université de Versailles Saint Quentin, 45 avenue des Etats-Unis, 78035 Versailles Cedex, France, and Materials Research Laboratory, University of California, Santa Barbara, California 93106-5121

Received: August 23, 2004; In Final Form: October 11, 2004

The transition-metal-incorporated nickel phosphate molecular sieves (TMI-VSB-5) have been hydrothermally synthesized at 453 K in weak basic conditions under microwave irradiation. By means of X-ray diffraction, inductively coupled plasma (ICP), ultraviolet−visible (UV−vis) diffuse reflectance, and Mössbauer spectroscopies, successful isomorphous (at least partial) substitution of transition-metal ions in the VSB-5 framework has been verified. Characterization results show that the framework structure of nanoporous VSB-5 can accommodate a substantial level of isomorphous substitution of transition-metal ions up to about 10, 5, and 3 atom % for Fe, Mn, and V, respectively, in both octahedral nickel sites (Mn and Fe) and tetrahedral phosphorus sites (V). The isomorphous substitution including the replacement mechanism was studied by not only the change of unit cell parameters but also spectroscopic analysis. The unit cell parameters of TMI-VSB-5 including a unit cell volume and *a*-axis length relied on the ionic radii difference between the incorporated ion and the original framework ions such as Ni or P ($R_{TMI} - R_{Ni}$ or $R_{TMI} - R_P$).

Introduction

The discovery of a large family of nanoporous aluminophosphates (AlPO-*n*)[1] in the early 1980s has generated widespread interest in non-aluminosilicate-based microporous materials, and there has been an enormous growth in the chemical diversity of open-framework phosphate materials in new compositional domains during the past decade.[2]

Metal-incorporated aluminophosphate molecular sieves (MeAPO-*n*)[3,4] and metal phosphates[2] have attracted considerable attention for applications in catalysis, adsorption, separations, and so forth. Isomorphous incorporation of transition-metal ions (TMIs) into the frameworks of porous materials such as zeolites and AlPO-*n* is very important because metal-incorporated molecular sieves contain atomically dispersed metal species and such sites may impart important redox and catalytic properties.[3−5] However, it has often been difficult to verify the metal incorporation into the framework by typical characterization methods because the amount of transition-metal ions incorporated is normally insufficient[3] to change the unit cell (UC) dimensions in a significant manner.[4,6,7] For example, despite a few studies verifying the metal substitution by X-ray absorption spectroscopy (XAS)/X-ray diffraction (XRD)[8] and electron spin−echo modulation (ESEM),[9] it is still debated whether the substitution site for TMIs is Al or P in several MeAPO-*n* materials.[3]

Recently, we have discovered the nanoporous nickel(II) phosphate molecular sieves VSB-1[10] and VSB-5,[11] which have very interesting properties. The VSB-5 structure (hexagonal, space group $P6_3/m$) that has several applications such as hydrogen storage[12] and selective catalysts[11] (for hydrogenation and base reactions) is based on a 1D 24-ring channels system, which consists of HPO_4, PO_4, and water molecules bound directly to octahedrally coordinated Ni^{2+}.[11] The structure of VSB-5 viewed down the *c*-axis is shown in Figure 1. The octahedral nickel and tetrahedral phosphorus are represented in green and purple, respectively. Its surface area and chemical composition are about 300−400 $m^2\ g^{-1}$ (after dehydration) and $Ni_{20}[(OH)_{12}(H_2O)_6][(HPO_4)_8(PO_4)_4]\cdot 12H_2O$, respectively. It is worth noting that the framework nickel atoms (in the VSB-5 structure) with octahedral coordination are different from those incorporated into AlPO and SAPO molecular sieves which have tetrahedral coordination, for example, Ni-SAPO-34.[13] In this work, we report new results of investigation on the isomorphous substitution of various TMIs into the VSB-5 framework, which have been confirmed by unit cell parameters, spectroscopy, and chemical analysis.

Experiment Section

The VSB-5 and transition-metal-incorporated VSB-5 (TMI-VSB-5) were hydrothermally synthesized with microwave irradiation, which imparts advantages of fast crystallization and phase selectivity.[14] A typical synthesis was carried out at 453 K for 4 h under weak basic conditions (pH 7−8) without any organic template.[15] The reactant composition was xTMI/$0.63H_3PO_4/1.0NiCl_2/3.0NH_3/100H_2O$.

In the synthesis using microwave heating, the reaction temperature was controlled using an EST-300 Plus system

* To whom correspondence should be addressed. E-mail: jschang@krict.re.kr (J.-S.C.); cheetham@mrl.ucsb.edu (A.K.C.). Fax: +82-42-860-7676 (J.-S.C.); +1-805-893-8797 (A.K.C.).
[†] Korea Research Institute of Chemical Technology.
[‡] Université du Maine.
[§] Université de Versailles Saint Quentin.
[||] University of California, Santa Barbara.

10.1021/jp046188g CCC: $30.25
Published on Web 12/21/2004

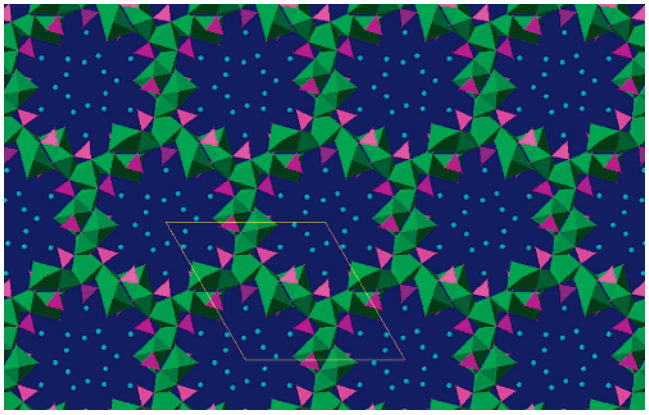

Figure 1. Representation of VSB-5 structure viewed down the *c*-axis, with octahedral nickel represented in green and tetrahedral phosphorus represented in purple.

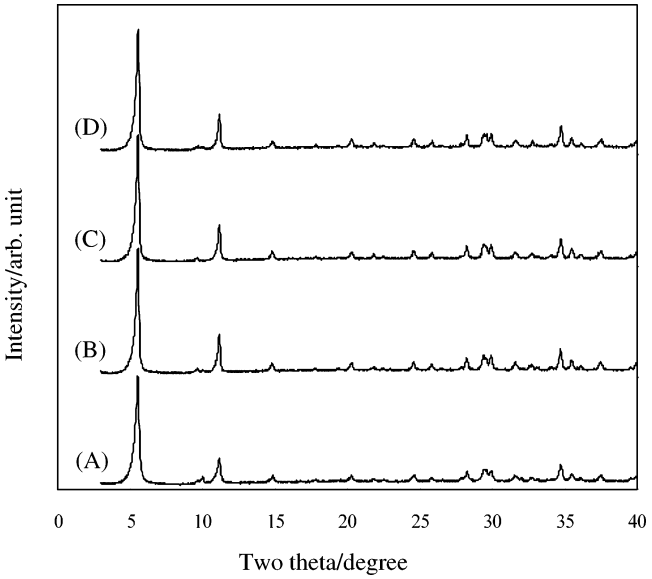

Figure 2. XRD patterns of as-synthesized VSB-5 and V-VSB-5. Parts A, B, C, and D correspond to sample numbers A, E, F, and G of Table 1, respectively. Fe-VSB-5 and Mn-VSB-5 show similar patterns.

(temperature control electronic sensor) that monitored and controlled the temperature conditions inside sample vessels. In this system, a microwave transparent fiberoptic temperature probe was inserted into a thermowell of a sample vessel. The temperature sensor was a phosphor located at the tip of the probe. The decay rate of fluorescent light emitted from the phosphor is temperature dependent, allowing a precise determination of temperature. For safety, the temperature of the reaction vessel in the microwave oven was measured using an optional TempGuard system. An infrared lens and sensor were located in the microwave oven, and the temperature of each vessel was measured as the vessels rotated over the sensor. If the temperature in any vessel was higher than the maximum preset temperature, the TempGuard stopped microwave generation.

The atomic concentration of added or incorporated TMI is reported in atom % on the basis of the total concentration of TMI, Ni, and P. The precursors for V, Fe, and Mn were $VOSO_4 \cdot 4H_2O$, $FeCl_2 \cdot 4H_2O$, and $Mn(OAc)_2 \cdot 4H_2O$ (all Aldrich), respectively. The UC dimension was calculated with a standard least-squares refinement technique, and α-alumina was used as an internal standard. Mössbauer experiments for iron species in Fe-VSB-5 were performed at 77 and 300 K using a constant acceleration mode spectrometer and a ^{57}Co source diffused into an Rh matrix. The isomer shifts are quoted relative to α-Fe at 300 K. The ultraviolet−visible (UV−vis) diffuse reflectance spectra (DRS) were recorded under ambient conditions using an UV−vis spectrophometer equipped with a quartz flat cell. The chemical compositions of the molecular sieves were determined using inductively coupled plasma (ICP).

Results and Discussion

The synthesized VSB-5 and TMI-VSB-5 molecular sieves are highly crystalline and have homogeneous morphologies (typically a rodlike shape), as illustrated in the XRD patterns and scanning electron microscopy (SEM) images (Figures 2 and 3). The crystallinity and morphology do not change substantially after the incorporation of transition-metal ions such as vanadium, iron, and manganese. The VSB-5 and TMI-VSB-5 have type I nitrogen adsorption−desorption isotherms (Figure 4), showing the characteristics of microporous materials. The Brunauer−Emmett−Teller (BET) surface areas of TMI-VSB-5 molecular sieves are in the range 320−350 m^2/g, which are almost the same as those of VSB-5 (Table 1). The pore volumes show

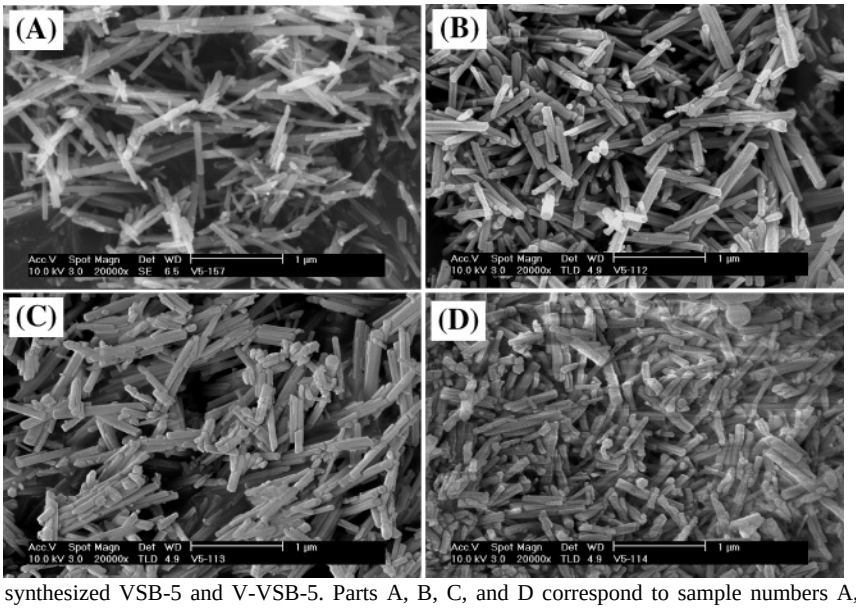

Figure 3. SEM image of synthesized VSB-5 and V-VSB-5. Parts A, B, C, and D correspond to sample numbers A, E, F, and G of Table 1, respectively. Fe-VSB-5 and Mn-VSB-5 show similar patterns.

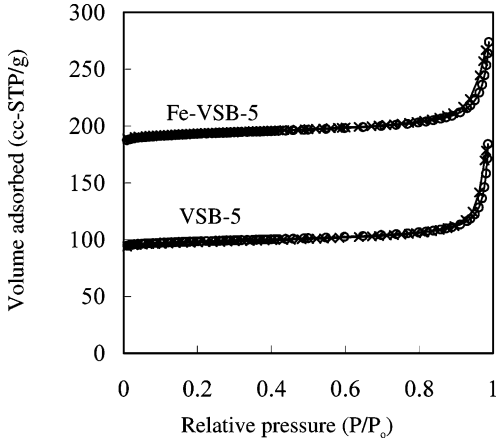

Figure 4. Nitrogen adsorption−desorption isotherms of VSB-5 (sample A) and Fe-VSB-5 (sample D). The circle and cross represent the adsorption and desorption isotherms, respectively, and the isotherms of Fe-VSB-5 are shifted upward by 100 cm^3/g for clearance. The other TMI-VSB-5 shows a similar adsorption−desorption isotherm.

similar results (Table 1). Moreover, the BET surface areas and pore volumes do not change noticeably after washing the TMI-VSB-5 with acidic solution (pH ∼ 2, aqueous HCl solution) to remove possible, if any, extraframework species. This may show that the major portions of TMIs in VSB-5 do not exist as extraframework species (that may be removed by acid washing) to decrease void space.[4]

The UC volumes decrease with increasing iron concentration, whereas the volumes increase with the concentrations of V and Mn, as shown in Figure 5. The *a*-axes exhibit a very similar trend to the change of UC volume, but the changes of *c*-axes are relatively small (Figure 5). Similar to the result of VAPO-5,[6] the *c*-axis in V-VSB-5 does not change with the V concentration. It has been pointed out that the formal charge and ionic radius are very important for the isomorphous substitution of a TMI in a molecular sieve.[3,16] Indeed, the increase of UC volumes would be reasonably explained by the assumption that vanadium (V^{4+}) and manganese (Mn^{2+}) substitute for phosphorus (P^{5+}) and nickel (Ni^{2+}), respectively, because $R_{V^{4+}}$ (0.48 Å) > $R_{P^{5+}}$ (0.17 Å) (ionic radii in 4-fold coordination) and $R_{Mn^{2+}}$ (0.83 Å) > $R_{Ni^{2+}}$ (0.69 Å) (ionic radii in 6-fold coordination).[17] The reverse cases that Mn replaces P and V replaces Ni should reveal the opposite trend to the present observed results, so that the possibility of a different substitution mechanism in Mn-VSB-5 and V-VSB-5 might be excluded. The steeper slope of V-VSB-5 compared with that of Mn-VSB-5 may be due to the larger difference of the ionic radii between V and P ($R_{V^{4+}} - R_{P^{5+}}$) than the difference between Mn and Ni ($R_{Mn^{2+}} - R_{Ni^{2+}}$).

On the contrary, the observed UC decrease for the Fe-VSB-5 is not in agreement with the expectation that Fe^{2+} might be incorporated in the nickel site in VSB-5 because $R_{Fe^{2+}}$ (0.78 Å) > $R_{Ni^{2+}}$ (0.69 Å). This inconsistency could be due to an oxidation process during the synthesis of the Fe-incorporated samples. To figure out the oxidation state of iron species in the Fe-VSB-5, Mössbauer experiments were performed on these samples. The isomer shift (IS) of iron has been used to characterize the oxidation state and symmetry of iron; from the IS values, the iron species can be easily assigned to one of the $Fe^{3+}(T_d)$, $Fe^{3+}(O_h)$, $Fe^{2+}(T_d)$, or $Fe^{2+}(O_h)$ species.[18,19] Table 2

TABLE 1: Reaction Conditions and Properties of TMI-VSB-5 Molecular Sieves Synthesized by the Microwave Method

sample no.[b]	reaction conditions			normalized compositions of TMI-VSB-5 (±0.3)[a]			S_{BET} [d] of TMI-VSB-5	pore volume of TMI-VSB-5 (cm^3/g)
	TMI	x[c]	TMI/(TMI + Ni + P) ratio[a]	TMI	Ni	P		
A		0.00	0.0	0.0	62.2	37.8	340	0.26
B	Fe	0.033	2.0	1.5	61.2	37.3	350	0.27
C	Fe	0.068	5.0	3.0	59.5	37.5	345	0.26
D	Fe	0.181	10.0	5.9	56.2	37.9	330	0.26
E	V	0.016	1.0	0.6	61.8	37.6	340	0.27
F	V	0.033	2.0	1.1	61.9	37.0	320	0.25
G	V	0.068	4.0	1.9	61.6	36.5	350	0.27
H	Mn	0.016	1.0	0.8	61.9	37.3	335	0.26
I	Mn	0.033	2.0	1.5	60.7	37.8	350	0.27
J	Mn	0.068	4.0	2.4	60.2	37.4	340	0.26

[a] Based only on the concentration of TMI, Ni, and P and the atomic %. [b] A, VSB-5; B−D, Fe−VSB-5; E−G, V−VSB-5; H−J, Mn−VSB-5. [c] *x* means the atomic ratio of TMI/Ni in reaction mixtures (xTMI/0.63H_3PO_4/1.0$NiCl_2$/3.0NH_3/100H_2O). [d] BET surface areas (m^2/g) of samples after evacuation at 300 °C.

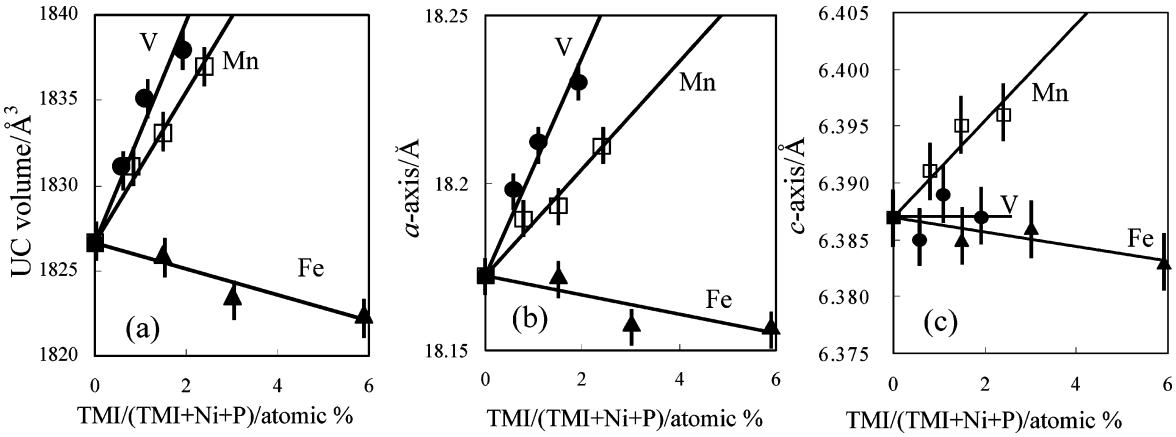

Figure 5. Changes of the UC dimensions of TMI-VSB-5 with the type and concentration of incorporated metal ions: (a) a unit cell volume; (b) *a*-axis length; (c) *c*-axis length.

TABLE 2: Refined Fitting Parameters for the Mössbauer Spectra of Fe-VSB-5 at 77 K (IS, Γ, and Δ Correspond to the Isomer Shift Quoted Relative to That of α-Fe at 300 K, Linewidth at Half-Height, and Quadrupolar Splitting, Respectively)

no.	IS (mm/s) (±0.01)	Γ (mm/s) (±0.01)	Δ (mm/s) (±0.02)	assigned species	proportion (%) (±1)
C	0.49	0.29	0.70	$Fe^{3+}(O_h)$	48
	0.49	0.29	0.91	$Fe^{3+}(O_h)$	46
	1.24	0.23	2.63	$Fe^{2+}(O_h)$	6
D	0.48	0.29	0.56	$Fe^{3+}(O_h)$	41
	0.49	0.38	0.90	$Fe^{3+}(O_h)$	56
	1.24	0.30	2.77	$Fe^{2+}(O_h)$	3

summarizes the coordination numbers and oxidation states of iron in Fe-VSB-5 with two different iron contents, as obtained from refined fitting parameters for the Mössbauer spectra at 77 K (Figure 6 for sample D). The spectra can be refined by three sets of quadrupolar doublets at 77 K.[20] Thanks to the IS values, the quadrupolar doublets are unambiguously attributed to two Fe^{3+} ions and one Fe^{2+} ion located in FeO_6 octahedral-like units. The presence of several components in Fe-VSB-5 is due to the occurrence of different cationic neighbors (Ni or Fe) close to Fe nuclei.[20] The Mössbauer results, therefore, demonstrate that the substitution of Ni^{2+} by Fe in VSB-5 is accompanied by a simultaneous oxidation of most of the Fe^{2+} into Fe^{3+} (>94%). Detailed Mössbauer results on the Fe-VSB-5 will be published elsewhere.[20] The oxidation of Fe^{2+} to Fe^{3+} in the synthesis of a porous material has also been reported in FAPO-5, FAPO-34, and FAPO-36.[4,18,21] The mean radius (R_{Fe} = ~0.652 Å) corresponding to the occupancy (95% Fe^{3+} and 5% Fe^{2+}) is then in agreement with the observed decrease of UC volume ($R_{Ni^{2+}}$ = 0.69 Å).

The effect of incorporated transition-metal ions on *a*-axis length among the UC parameters is illustrated quantitatively in Figure 7. The change of *a*-axis length correlates obviously with the difference of ionic radii of TMI (for Fe and Mn) and Ni or TMI (for V) and P, showing that the *a*-axis length increases linearly with the bond length of TMI−O replacing Ni−O or P−O regardless of the type of TMI. The UC volume shows a similar trend to that of the *a*-axis (data not shown). However, the UC volumes of V-VSB-5 show a slightly decreased dependence (from the linear plot obtained from the UC volumes of Fe-VSB-5, VSB-5, and Mn-VSB-5) on the ionic radii

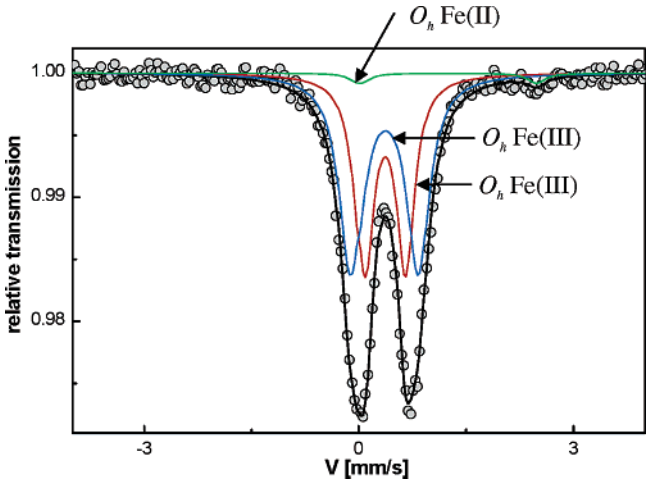

Figure 6. Mössbauer spectra (black) of Fe-VSB-5 (sample D) at 77 K fitted with three quadrupolar doublets. The two contributions of $Fe^{3+}(O_h)$ are in red and blue; those of $Fe^{2+}(O_h)$ are in green. The relative contents of Fe^{3+} and Fe^{2+} in the Fe-VSB-5 can be assigned to 97 and 3%, respectively, according to this spectrum.

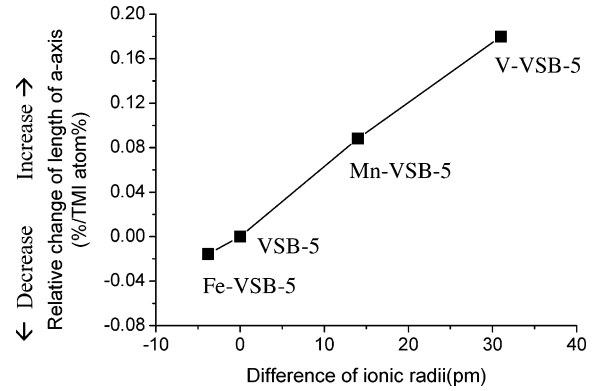

Figure 7. Change of *a*-axis length (per unit atomic % of TMI) in the unit cell of TMI-VSB-5 with the difference of ionic radii between TMI and Ni (or P). For example, the *a*-axis length increases ~0.18% when TMI replaces 1% of (Ni + P) and the difference of ionic radii is 30 pm. The difference of ionic radii means $R_{TMI} - R_{Ni}$ (for Fe and Mn) or $R_{TMI} - R_P$ (for V). Each data point corresponds to Fe-VSB-5 ($R_{Fe^{3+/2+}} - R_{Ni^{2+}}$), VSB-5 itself, Mn-VSB-5 ($R_{Mn^{2+}} - R_{Ni^{2+}}$), and V-VSB-5 ($R_{V^{4+}} - R_{P^{5+}}$) from left to right.

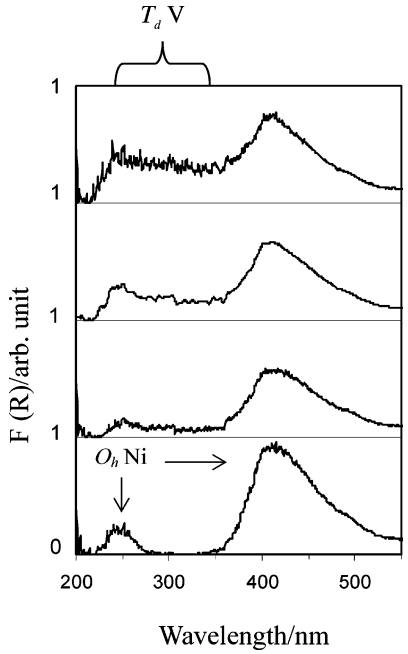

Figure 8. UV−vis DRS spectra of synthesized V-VSB-5 with the concentration of TMI. The concentrations increase from bottom to top. The lowest spectrum corresponds to the VSB-5 without any TMI.

difference, which may show the contribution of V^{5+} (see below) due to $R_{V^{4+}} > R_{V^{5+}}$. These results demonstrate that the change of UC dimensions (volume and *a*-axis) depends mainly on the ionic radii differences ($R_{Fe^{3+/2+}} - R_{Ni^{2+}}$, $R_{Mn^{2+}} - R_{Ni^{2+}}$, or $R_{V^{4+/5+}} - R_{P^{5+}}$) between the incorporated metal ions and Ni or P.

It has been well-known that the UV absorption wavelength of vanadium increases with the coordination number of vanadium from 4 to 6; tetrahedral-like vanadium shows maximum absorption below ~333 nm, and octahedral-like vanadium shows maximum absorption above ~333 nm.[6,22−24] For more precise assignments, it has also been reported that the four-coordinated V^{4+} and four-coordinated V^{5+} have absorbance bands at about 240−285 and 285−335 nm, respectively.[22,23] The experimental absorption spectra of V-VSB-5 (Figure 8) are mainly indicative of tetrahedral-like vanadium. Moreover, from the UV−vis DRS spectra, the presence of V^{5+} cannot be excluded because of the

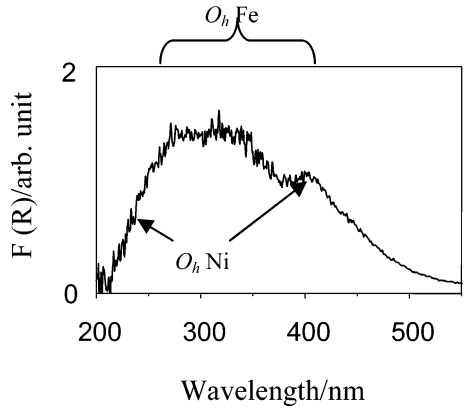

Figure 9. UV−vis DRS spectra of Fe-VSB-5 (sample D of Table 1).

presence of absorption larger than 285 nm, similar to the oxidation of Fe^{2+} to Fe^{3+} and V^{4+} to V^{5+} reported in the synthesis of V-MCM-41.[25] Preliminary X-ray photoelectron spectroscopy (XPS) study shows the coexistence of V^{4+} and V^{5+} in V-VSB-5 even though the content of each component cannot be estimated precisely due to the overlap of V2p and O1s (satellite spectrum) peaks. This UV−vis DRS result means that tetrahedral-like vanadium species principally substitute for phosphorus in the framework. There are a few articles that report the presence of *Td* V^{4+} [22,26−28] even though the tetrahedral V^{4+} is seldom due to the energetic instability. Moreover, the substitution of P by V has been expected or observed in the V-containing AlPO-*n* and a mineral called schoderite due to the similarities in the chemistry and charge of V and P.[4,29−32]

The octahedral-like symmetry of Fe^{3+} in Fe-VSB-5 has also been confirmed by UV−vis spectroscopic analysis (Figure 9). The UV absorption bands due to the charge transfer of the Fe^{3+}-(O_h) ion at around 278, 333, and 427 nm are known to be assigned to the isolated Fe^{3+}, small clusters, and Fe_2O_3, respectively.[33] The absorption bands at around 215 and 241 nm correspond to $t_1 \rightarrow t_2$ and $t_1 \rightarrow e$ transitions of $Fe^{3+}(T_d)$, respectively.[33] The UV−vis DRS spectra of Fe-VSB-5 show very broad bands in the range 200−400 nm, quite different from those of $Fe^{3+}(T_d)$ present in Fe-ZSM-5, which exhibit an absorption maximum below 225 nm.[33] This result strongly suggests that the main contribution in Fe-VSB-5 concerns Fe^{3+} ions in octahedral-like coordination and therefore they principally substitute for octahedral nickel sites in VSB-5.

The substitution sites for the TMI can be further verified by chemical analysis using ICP, as shown in Table 1. The normalized chemical compositions of both Fe-VSB-5 and Mn-VSB-5 materials exhibit a steady decrease of Ni concentration with increasing Fe or Mn concentration, demonstrating that the Fe and Mn ions principally substitute for Ni sites in VSB-5. The slight decrease of P with increasing V concentration indicates the substitution of P by V in V-VSB-5, although the existence of nonframework vanadium cannot be excluded because of the very slight decrease of Ni concentration with the incorporation of V. The incorporation limits for Fe, Mn, and V in VSB-5 are approximately 10, 5, and 3 atom %, respectively, based on the normalized compositions of TMI, Ni, and P.

Further studies are in progress to explore the catalytic properties of TMI-VSB-5 for elucidating the role of transition-metal ions isomorphously substituted in the framework of VSB-5 in the field of redox catalysis. Moreover, the charge balancing due to the substitution of Ni(II) with TMI(III) or P(V) with TMI(IV) will be explored further to confirm the substitution mechanisms even though it is expected that NH_4^+ and OH^- may be used for charge compensation because of the weak basic reaction condition using aqueous ammonia.

Conclusions

The isomorphous (at least partial) substitution of various transition-metal ions with not only octahedral-like (in the Ni sites) but also tetrahedral-like (in the P sites) symmetry in VSB-5 is found by UC parameters, spectroscopy, and chemical analysis. This work demonstrates that nanoporous VSB-5 has a versatile framework to accommodate various TMIs with several oxidation states and symmetries. Further studies are in progress to explore the catalytic properties of TMI-VSB-5 for elucidating the role of transition-metal ions isomorphously substituted in the framework of VSB-5 in the field of redox catalysis.

Acknowledgment. This work was supported by the Korea Ministry of Science and Technology through the Research Center for Nanocatalysis and International Collaboration program and the MRSEC program of the National Science Foundation under Award No. DMR00-80034. The authors thank Professor S.-E. Park, Profl. Y.-U. Kwon, Mr. P. M. Forster, and Mr. J. W. Yoon for their beneficial contributions.

References and Notes

(1) Wilson, S. T.; Lok, B. M.; Messina, C. A.; Cannan, T. R.; Flanigen, E. M. *J. Am. Chem. Soc.* **1982**, *104*, 1146.

(2) (a) Cheetham, A. K.; Férey, G.; Loiseau, T. *Angew. Chem., Int. Ed.* **1999**, *38*, 3268 and references therein. (b) Rao, C. N. R.; Natarajan, S.; Neeraj, S. *J. Am. Chem. Soc.* **2000**, *122*, 2810. (c) Rao, C. N. R.; Natarajan, S.; Choudhury, A.; Neeraj, S.; Ayi, A. A. *Acc. Chem. Res.* **2001**, *34*, 80 and references therein.

(3) Hartmann, M.; Kevan, L. *Chem. Rev.* **1999**, *99*, 635 and references therein.

(4) Weckhuysen, B. M.; Rao, R. R.; Martens, J. A.; Schoonheydt, R. A. *Eur. J. Inorg. Chem.* **1999**, 565 and references therein.

(5) (a) Davis, M. E. *Nature* **2002**, *417*, 813 and references therein. (b) Thomas, J. M.; Raja, R.; Sankar, G.; Bell, R. G. *Acc. Chem. Res.* **2001**, *34*, 191 and references therein. (c) De Vos, D. E.; Sels, B. F.; Jacobs, P. A. *Adv. Synth. Catal.* **2003**, *345*, 457 and references therein. (d) Panov, G. I. *Cattech* **2000**, *4*, 18 and references therein. (e) Matsuoka, M.; Anpo, M. *J. Photochem. Photobiol. C* **2003**, *3*, 225 and references therein.

(6) Blasco, T.; Concepcióén, P.; Nieto, J. M.; Prez-Pariente, J. *J. Catal.* **1995**, *152*, 1.

(7) Canesson, L.; Tuel, A. *Zeolites* **1997**, *18*, 260.

(8) Thomas, J. M. *Angew. Chem., Int. Ed.* **1999**, *38*, 3588 and references therein.

(9) Prakash, A. M.; Hartmann, M.; Zhu, Z.; Kevan, L. *J. Phys. Chem. B* **2000**, *104*, 1610.

(10) (a) Guillou, N.; Gao, Q.; Nogues, M.; Morris, R. E.; Hervieu, M.; Férey, G.; Cheetham, A. K. *Acad. Sci. Paris* **1999**, *2*, 387. (b) Chang, J.-S.; Park, S.-E.; Gao, Q.; Férey, G.; Cheetham, A. K. *Chem. Commun.* **2001**, 859. (c) Chang, J.-S.; Hwang, J.-S.; Jhung, S. H.; Park, S.-E.; Férey, G.; Cheetham, A. K. *Angew. Chem., Int. Ed.* **2004**, *43*, 2819. (d) Jhung, S. H.; Chang, J.-S.; Yoon, J. W.; Grenèche, J.-M.; Férey, G.; Cheetham, A. K. *Chem. Mater.* **2004**, *16*, 5552.

(11) Guillou, N.; Gao, Q.; Forster, P. M.; Chang, J.-S.; Noguès, M.; Park, S.-E.; Férey, G.; Cheetham, A. K. *Angew. Chem., Int. Ed.* **2001**, *40*, 2831.

(12) Forster, P. M.; Eckert, J.; Chang, J.-S.; Park, S.-E.; Férey, G.; Cheetham, A. K. *J. Am. Chem. Soc.* **2003**, *125*, 1309

(13) Inoue, M.; Dhupatemiya, P.; Phatanasri, S.; Inui, T. T. *Microporous Mesoporous Mater.* **1999**, *28*, 19.

(14) (a) Arafat, A.; Jansen, J. C.; Ebaid, A. R.; van Bekkum, H. *Zeolites* **1993**, *13*, 162. (b) Park, M.; Komarneni, S. *Microporous Mesoporous Mater.* **1998**, *20*, 39. (c) Cundy, C. S.; Plaisted, R. J.; Zhao, J. P. *Chem. Commun.* **1998**, 1465. (d) Park, S.-E.; Chang, J.-S.; Hwang, Y. K.; Kim, D. S.; Jhung, S. H.; Hwang, J. S. *Catal. Surv. Asia* **2004**, *8*, 91 and references therein.

(15) Jhung, S. H.; Chang, J.-S.; Park, S.-E.; Forster, P. M.; Férey, G.; Cheetham, A. K. *Chem. Mater.* **2004**, *16*, 1394.

(16) (a) Martens, J. A.; Jacobs, P. A. *Stud. Surf. Sci. Catal.* **1994**, *85*, 653 and references therein. (b) Wilson, S. T. *Stud. Surf. Sci. Catal.* **2001**, *137*, 229 and references therein. (c) Feng, P.; Bu, X.; Stucky, G. D. *Nature* **1997**, *388*, 735.

(17) Shannon, R. *Acta Crystallogr.* **1976**, *A32*, 751. The ionic radii were as follows: $Ni^{2+}(O_h)$, 0.69 Å; $P^{5+}(T_d)$, 0.17 Å; $V^{4+}(T_d)$, 0.48 Å; $V^{5+}(T_d)$,

0.355 Å; $Fe^{2+}(O_h)$, 0.78 Å; $Fe^{3+}(O_h)$, 0.645 Å; $Mn^{2+}(O_h)$, 0.83 Å. The ionic radius of $V^{4+}(T_d)$ was estimated by the tendency with the coordination number of V^{4+}.

(18) Ristić, A.; Tušar, N. N.; Arčon, I.; Thibault-Starzyk, F.; Hanžel, D.; Czyzniewska, J.; Kaučič, V. *Microporous Mesoporous Mater.* **2002**, *56*, 303.

(19) (a) Ratnasamy, P.; Kumar, R. *Catal. Today* **1991**, *9*, 329. (b) Pérez-Ramírez, J.; Mul, G.; Kapteijn, F.; Moulijn, J. A.; Overweg, A. R.; Doménech, A.; Ribera, A.; Arends, I. W. C. E. *J. Catal.* **2002**, *207*, 113.

(20) Grenèche, J.-M.; Jhung, S. H.; Chang, J.-S.; Férey, G.; Cheetham, A. K. Manuscript to be submitted for publication.

(21) (a) Ristić, A.; Tušar, N. N.; Arčon, I.; Logar, N. Z.; Thibault-Starzyk, F.; Czyzniewska, J.; Kaučič, V. *Chem. Mater.* **2003**, *15*, 3643. (b) Park, J. W.; Chon, H. *J. Catal.* **1992**, *133*, 159.

(22) Centi, G.; Perathoner, S.; Trifiró, F.; Aboukais, A.; Aïssi, C. F.; Guelton, M. *J. Phys. Chem.* **1992**, *96*, 2617.

(23) Corma, A.; Nieto, J. M. L.; Paredes, N. *Appl. Catal., A* **1993**, *104*, 161.

(24) (a) Dzwigaj, S.; Matsuoka, M.; Anpo, M.; Che, M. *J. Phys. Chem. B* **2000**, *104*, 6012. (b) Jhung, S. H.; Uh, Y. S.; Chon, H. *Appl. Catal.* **1990**, *62*, 61. (c) Mathieu, M.; Voort, P. V. D.; Weckhuysen, B. M.; Rao, R. R.; Catana, G.; Schoonheydt, R. A.; Vansant, E. F. *J. Phys. Chem. B* **2001**, *105*, 3393.

(25) Chao, K. J.; Wu, C. N.; Chang, H.; Lee. L. J.; Hu, S.-F. *J. Phys. Chem. B* **1997**, *101*, 6341.

(26) Gregorio, S. D.; Greenblatt, M.; Pifer, J. H.; Sturge, M. D. *J. Chem. Phys.* **1982**, *76*, 2931.

(27) Liu, G.; Greedan, J. E. *J. Solid State Chem.* **1994**, *108*, 371.

(28) Anpo, M.; Higashimoto, S.; Matsuoka, M.; Zhanpeisov, N.; Shioya, Y.; Dzwigaj, S.; Che, M. *Catal. Today* **2003**, *78*, 211.

(29) Hausen, D. M. *Am. Mineral.* **1962**, *47*, 637.

(30) Prakash, A. M.; Kevan, L. *J. Phys. Chem. B* **1999**, *103*, 2214.

(31) Montes, C.; Davis, M. E.; Murray, B.; Narayana, M. *J. Phys. Chem.* **1990**, *94*, 6431.

(32) Zahedi-Niaki, M. H.; Zaidi, S. M. J.; Kaliaguine, S. *Appl. Catal., A* **2000**, *196*, 9.

(33) (a) Bordiga, S.; Buzzoni, R.; Geobaldo, F.; Lamberti, C.; Giamello, E.; Zecchina, A.; Leofanti, G.; Petrini, G.; Tozzola, G.; Vlaic, G. *J. Catal.* **1996**, *158*, 486. (b) Ribera, A.; Arends, I. W. C. E.; de Vries, S.; Pérez-Ramírez, J.; Sheldon, R. A. *J. Catal.* **2000**, *195*, 287.